Wavelength and position tuning of erenkov second-harmonic generation in optical superlattice

Ksawery Kalinowski, Qian Kong, Vito Roppo, Ady Arie, Yan Sheng et al.

Related Articles

Cascaded erenkov third-harmonic generation in random quadratic media
Appl. Phys. Lett. 99, 241109 (2011)

Time-resolved femtosecond optical characterization of multi-photon absorption in high-pressure-grown Al0.86Ga0.14N single crystals
J. Appl. Phys. 110, 113112 (2011)

Experimental observation of optical vortex in self-frequency-doubling generation
Appl. Phys. Lett. 99, 241102 (2011)

Model for nanosecond laser induced damage in potassium titanyl phosphate crystals
Appl. Phys. Lett. 99, 231111 (2011)

Direct comparison of phase-sensitive vibrational sum frequency generation with maximum entropy method: Case study of water
J. Chem. Phys. 135, 224701 (2011)

Additional information on Appl. Phys. Lett.

Journal Homepage: http://apl.aip.org/

Journal Information: http://apl.aip.org/about/about_the_journal

Top downloads: http://apl.aip.org/features/most_downloaded

Information for Authors: http://apl.aip.org/authors

Wavelength and position tuning of Čerenkov second-harmonic generation in optical superlattice

Ksawery Kalinowski,[1] Qian Kong,[2,3] Vito Roppo,[4] Ady Arie,[5] Yan Sheng,[1,2,a] and Wieslaw Krolikowski[2]

[1]*Laser Physics Center and Nonlinear Physics Center, Research School of Physics and Engineering, Australian National University, Canberra ACT 0200, Australia*
[2]*Laser Physics Center, Research School of Physics and Engineering, Australian National University, Canberra ACT 0200, Australia*
[3]*Department of Physics, Shanghai University, Shanghai 200444, China*
[4]*Departament de Fisica i Enginyeria Nuclear, Universitat Politecnica de Catalunya, Rambla Sant Nebridi, 08222 Terrassa, Spain*
[5]*Department of Physical Electronics, Faculty of Engineering, Tel Aviv University, Tel Aviv 69978, Israel*

We study experimentally the Čerenkov second-harmonic generation in an optical superlattice formed in periodically poled lithium niobate crystal. We demonstrate strong sensitivity of the Čerenkov signal to the wavelength, diameter, and position of the incident fundamental beam. We model the observed behavior by using simple approach based on multiple interference of second harmonic signals emitted from the vicinity of the domain walls. © *2011 American Institute of Physics*. [doi:10.1063/1.3659493]

Čerenkov second harmonic generation (SHG) represents the interesting type of nonlinear interaction where the second harmonic (SH) is emitted at the so-called Čerenkov angle with respect to the propagation direction of the fundamental wave.[1] Different from the classical phase matched SHG (Refs. 2 and 3), the Čerenkov SHG requires only the longitudinal components of the momenta of the fundamental and SH waves to match, i.e., $k_2 \cos\theta = 2k_1$, with k_1 and k_2 denoting the wave vectors of the fundamental and SH waves and θ being the Čerenkov angle (Fig. 1).

Originally the Čerenkov SHG was intensively studied in waveguide geometries utilizing the automatically fulfilled Čerenkov condition with the fundamental beam propagating as a guided mode and the SH as the substrate radiation modes, respectively.[4,5] Recently, this type of SHG has been demonstrated in bulk materials with spatial modulation of second-order nonlinearity, including one-dimensional optical superlattice[6–8] and two-dimensional nonlinear photonic crystals.[9] It was observed that the emission pattern of the Čerenkov SHG in bulk materials depends on polarization state[10,11] as well as the propagation direction[12] of the fundamental waves. It is also established that the presence of spatial $\chi^{(2)}$ modulation can greatly enhance the intensity of the Čerenkov SHG,[13] owing possibly either to the reciprocal lattice vectors (RLV) of nonlinear structure or the enhanced quadratic nonlinearity on the vicinity of domain walls.[6,8]

While the Čerenkov SHG has been studied in bulk materials for some time, its tuning response to a range of parameters, e.g., wavelength and position of the incident beam, has not been investigated so far. In this letter, we study experimentally the Čerenkov SH emission in periodically poled lithium niobate (PPLN) crystal. We reveal that, in contrast to the classic SHG whose tuning response is determined by the superlattice itself (i.e., its periodicity), the sensitivity of the

Čerenkov harmonic emission to the wavelength/position tuning depends strongly on the width of the fundamental beam. We explain this phenomenon by employing a simplified theoretical model that takes into account the interference among the constituent Čerenkov SH signals generated on domain walls.

In our experiments (Fig. 1), we use z-cut PPLN crystal (nominal period $\Lambda = 14.6\ \mu$m, duty cycle $D \approx 50\%$, thickness $L \approx 500\ \mu$m). The fundamental wave is generated by a femtosecond MIRA (Coherent) oscillator which is tuned from 805 to 840 nm, with the pulse duration 180 fs and repetition rate 76 MHz and average power 200 mW. The laser beam propagates along the z-axis of the sample and is focused subsequently by microscope objectives ($100\times$ and $10\times$) and optical lens (40 mm and 200 mm focal-lengths). The estimated resulting diameters of the focal spots at the surface of the sample (in the air) are 2 μm, 5 μm, 15 μm, and 77 μm, respectively. In order to change relative position of the beam center with respect to domain walls, the sample is mounted
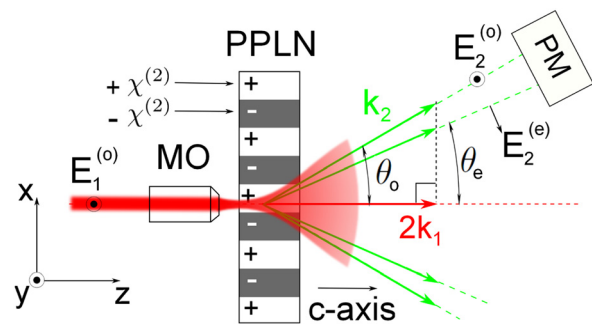

FIG. 1. (Color online) Experimental setup and the phase-matching diagram of Čerenkov second harmonic generation. E_1 and E_2 represent amplitudes of the incident fundamental and emitted second harmonics, respectively. q denotes the phase mismatch, MO—microscope objective, and PM—detector. θ_o and θ_e denote emission angles of the ordinary $(E_2^{(O)})$ and extraordinary $(E_2^{(e)})$ Čerenkov signals, respectively.

[a]Electronic mail: ysh111@physics.anu.edu.au.

on a translational stage which can be positioned in x-direction with 100 nm step.

We observe two pairs of Čerenkov SH spots with orthogonal polarization directions (Fig. 1) emitted non-collinearly and symmetrically with respect to the direction of the fundamental beam in the plane perpendicular to the domain wall (see also Fig. 2 in Ref. 13). The size of the generated Čerenkov beams in the near field corresponds to the spatial extent of the fundamental beam. Since the fundamental beam is ordinarily polarized, we identify the interactions that are responsible for the SH spots as $o_1 + o_1 \rightarrow e_2$ and $o_1 + o_1 \rightarrow o_2$. The measured emission angle (in air) is $\theta_e = 55.67°$ for the extraordinary SHG, and $\theta_o = 59.70°$ for the ordinary one. These angles agree well with the theoretical values $\theta_e = 55.97°$ and $\theta_o = 59.94°$ obtained by using the reported refractive index of LiNbO$_3$ crystal.[14] The measured maximum conversion efficiency for the $o_1 + o_1 \rightarrow e_2$ interaction is 1.1×10^{-7} and for the $o_1 + o_1 \rightarrow o_2$ interaction is from 2 to 4 times lower (depending on the wavelength). In Fig. 2, we depict normalized intensity of the total Čerenkov signal vs. wavelength of the fundamental beam and its lateral position for different values of the beam diameter. In all measurements, the average power of the fundamental wave was kept constant ($\sim$200 mW). It is clearly seen that the Čerenkov SH signal strongly depends on the beam width of the fundamental wave. When the beam is tightly focused [Fig. 2(a)], the Čerenkov SHG only weakly depends on the wavelength but changes drastically with the incident position of the fundamental beam. In fact, the Čerenkov emission takes place only when the tightly focussed fundamental wave is incident at the domain wall separating regions of positive and negative $\chi^{(2)}$. This unique property of Čerenkov emission forms a basis of a nonlinear microscopy for visualizing ferroelectric domain structures.[7,13] Now, the graph [Fig. 2(a)] confirms that such type microscopy can operate at any wavelength as long as the beam width is small enough to cover a single domain wall only. When the incident fundamental beam is broader [Figs. 2(b) and 2(c)], the Čerenkov SHG becomes sensitive to both position and the wavelength. One can clearly observe now smoothing out of previously

sharp position-dependent features and, at the same time, strong dependence on the input wavelength. For very broad input beam, the emitted SH shows basically only the wavelength dependence [Fig. 2(d)].

In order to explain these observations note that the efficient Čerenkov SHG takes place only in the vicinity of the domain walls [see Fig. 2(a)]. We believe that the actual physical reason of this effect is the abrupt change of the sign of nonlinearity which serves as a source of reciprocal vectors enabling efficient phase matching of the SHG.[3] For a tightly focused fundamental beam [see Fig. 3(a)], the only source of the Čerenkov signal is the domain wall that is covered by the beam (position A). Therefore, if we shift such narrow beam away from the wall towards a homogenous domain (i.e., position B), we will observe strong variation of the SH signal (from maximum to almost null). Situation is entirely different when the fundamental beam is broad such that it illuminates few domain walls [see Fig. 3(b)]. Since the beam width is large compared to periodicity of the nonlinear superlattice, shifting its position does not change substantially the number of domain walls involved in the SH generation [Fig. 3(b)]. As a result, the strength of the Čherenkov SHG changes little with the beam position.

Totally different is the wavelength sensitivity of the Čerenkov signal originating from narrow and wide beams. As the SH emission is only determined by the effective nonlinearity which is almost constant in a broad range of wavelengths for a very narrow beam that can cover a single domain wall, the Čerenkov signal emitted by this beam does not depend on the wavelength. On the other hand, for wide fundamental beam, the Čerenkov signal arises as a superposition of the partial signals generated on all domain walls covered by the beam. Because of oblique emission, the constituent signals differ in phase which depends on the wavelength of the fundamental beam and so the total Čerenkov signal becomes wavelength-dependent as well. One can also look at this effect by considering the role of RLV in Fourier space. It is known that the Čerenkov SHG is longitudinally phase-matched and there is a phase mismatch q in transverse x direction. For a wide fundamental beam, the modulation of the nonlinearity is spatially periodic providing RLV $G_m = 2m\pi/\Lambda$ ($m = 1, 2,\ldots$) to the Čerenkov interaction. The emission is expected to be the strongest at the wavelengths where the phase mismatch is completely compensated by the
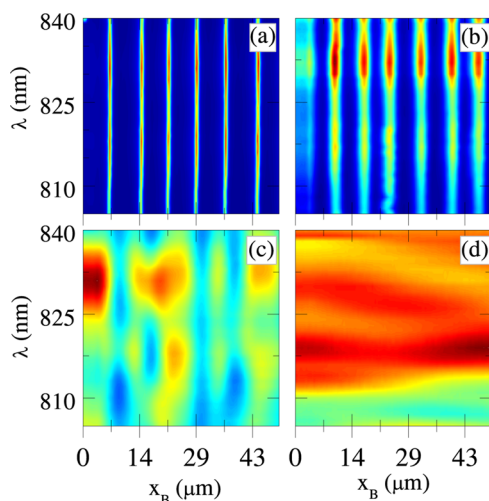

FIG. 2. (Color online) Measured Čerenkov SH signal as functions of wavelength and incidence position for different widths of the fundamental beam. From (a) to (d), the beam width is 2 μm, 5 μm, 15 μm, and 77 μm.
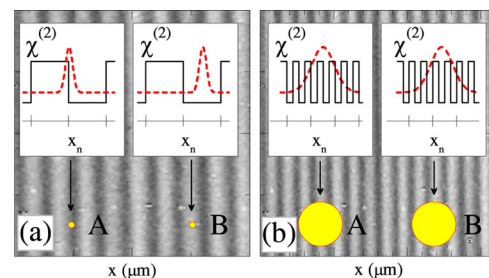

FIG. 3. (Color online) Schematically shown position of the beam (yellow dots) against the background of the domains. Insets show the spatial beam profile (red dashed lines) with respect to $\chi^{(2)}$ modulation (gray solid lines) for (a) tightly focused beam where beam overlaps with a domain wall (left inset) or in the middle of the domain (right inset), (b) the same but for wide beam.
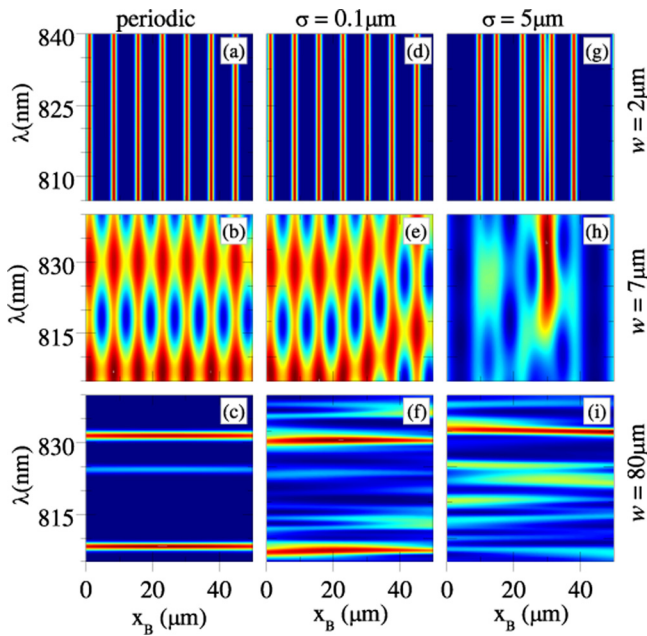
FIG. 4. (Color online) Calculated [see Eq. (1)] intensity of the Čerenkov SH as functions of the wavelength and position of the fundamental beam for different beam widths (columns) and degree of disorder of the structure represented by the dispersion (σ) of the domain widths (rows).

RLV, i.e., $q(\lambda) = k_2 \sin \theta = G_m$. However, the considerations above do not apply to the Čerenkov SHG for a very narrow beam, as such beam cannot feel the periodic modulation of nonlinearity at all [Fig. 3(a)]. In this case, the RLV is either presented by a single domain wall when the beam is exactly located on the wall (Position A in Fig. 3(a)), or there are no RLV at all when the beam is tuned away from the wall (position B). These two situations change little with the wavelength, so does the Čerenkov SHG. It is worth noting that slight wavelength dependence of the Čerenkov signal is still observed in experiment for a very narrow beam [Fig. 2(a)], which can be attributed to strong diffraction suffered by the fundamental beam. For example, a spot of 2 μm diameter may grow as large as $\sim$300 μm at the end of the crystal (where the Rayleigh range is 32 μm) and hence cover many domains. However, we believe the nonlinear contribution is still mainly from the first part in which the beam is smaller than a domain, as after that the pump intensity drops significantly. To model the observed phenomenon, we use very simple model which treats the Čerenkov emission as a result of coherent superposition of the constituent signals generated on the successive domain walls.[15] Then the intensity of the Čerenkov signal I_2 can be represented as

$$I_2(\lambda, x_B) \propto \left| \frac{1}{\lambda n_2} \sum_{n=1}^{N} E_1^2(x_n) e^{-i(k_2 x_n \sin \theta + n\pi)} \right|^2, \quad (1)$$

where x_n is the coordinate of the nth domain wall, N is the number of domain walls, and $E_1(x_n)$ is the electric field of the fundamental wave at nth domain wall and for Gaussian beam it reads $E_1^2(x_n) = e^{-4\ln 2(x_n - x_B)2/w^2}$. The π shift between neighboring components in the Eq. (1) reflects the change of

the sign of nonlinearity across the domain wall. Fig. 4 depicts the calculated normalized Čerenkov intensity for different beam width and wavelength using Eq. (1). Graphs in the left column depict emission from the perfectly periodic structure ($\Lambda = 14.6$ μm). It is seen that the simulation correctly replicates the behavior of Čerenkov emission in the sense that for tightly focused beam [Fig. 4(a)] the emission exhibits strong position sensitivity while being completely independent on the wavelength and opposite in case of large beam size [Fig. 4(c)]: the emission exhibits strong wavelength sensitivity while being completely independent of the beam position. The visible discrepancy between experiment and theory is caused by the assumption of an ideal periodic superlattice in the latter. As can be seen on the graph in Fig. 2(a), our fabricated structure is in fact not exactly periodic. Moreover, it appears that the duty cycle randomly varies inside the sample. These factors can easily deviate Čerenkov SH emission pattern from expected one. Graphs in the middle and right columns in Fig. 4 illustrates calculated Čerenkov signal assuming randomized spatial domain distribution with an average domain size of $\Lambda/2 = 7.3$ μm and different dispersions of $\sigma = 0.1$ μm (middle column) and $\sigma = 5$ μm (right column). The deterioration of the emission spectra is evident.

In conclusion, we have studied the Čerenkov SHG in a periodically poled LiNbO$_3$ crystal. We found that the tuning response of the Čerenkov emission to the wavelength and the position of the fundamental beam depend strongly on the beam width. Our study contributes to a deeper understanding of the nonlinear Čerenkov emission. It is also important for utilizing the Čerenkov interaction in applications for high resolution nonlinear microscopy and light sources including terahertz radiations.

[1]A. Zembrod, H. Puell, and J. A. Giordmaine, Opt. Quantum Electron. **1**, 64 (1969).
[2]J. A. Giordmaine, Phys. Rev. Lett. **8**, 19 (1962).
[3]J. A. Amstrong, N. Bloembergen, J. Ducuing, and P. S. Pershan, Phys. Rev. **127**, 1918 (1962).
[4]P. K. Tien, R. Ulrich, and R. J. Martin, Appl. Phys. Lett. **17**, 447 (1970).
[5]Y. Zhang, Z. D. Gao, Z. Qi, S. N. Zhu, and N. B. Ming, Phys. Rev. Lett. **100**, 163904 (2008).
[6]A. Fragemann, V. Pasiskevicius, and F. Laurell, App. Phys. Lett. **85**, 375 (2004).
[7]X. Deng and X. Chen, Opt. Express **18**, 15597 (2010).
[8]X. Deng, H. Ren, Y. Zheng, K. Liu, and X. Chen, e-print arXiv:1005.2925.
[9]S. M. Saltiel, Y. Sheng, N. Voloch-Bloch, D. N. Neshev, W. Krolikowski, A. Arie, K. Koyonov, and Y. S. Kivshar, IEEE J. Quantum Electron. **45**, 1465 (2009).
[10]Y. Sheng, S. M. Saltiel, W. Krolikowski, A. Arie, K. Koynov, and Y. Kivshar, Opt. Lett. **35**, 1317 (2010).
[11]P. Molina, M. O. Ramirez, B. J. Garcia, and L. E. Bausa, Appl. Phys. Lett. **96**, 261111 (2010).
[12]W. Wang, Y. Sheng, Y. Kong, A. Arie, and W. Krolikowski, Opt. Lett. **35**, 3790 (2010).
[13]Y. Sheng, A. Best, H. Butt, W. Krolikowski, A. Arie, and K. Koynov, Opt. Express **16**, 16539 (2010).
[14]G. J. Edwards and M. Lawrence, Opt. Quantum Electron. **16**, 373 (1984).
[15]H. Ren, X. Deng, and X. Chen, e-print arXiv:1010.1593v1.